2006

Electrochemically Modulated Permeability of Poly(aniline) and Composite Poly(aniline)–Poly(styrenesulfonate) Membranes

D. L. Pile
Iowa State University

Y. Zhang
Iowa State University

Andrew C. Hillier
Iowa State University, hillier@iastate.edu

Electrochemically Modulated Permeability of Poly(aniline) and Composite Poly(aniline)–Poly(styrenesulfonate) Membranes

Abstract
The influence of oxidation state on the permeability of several probe molecules through conducting polymer membranes comprising composites of poly(aniline) and poly(styrenesulfonate) was examined in aqueous solution. Pure poly(aniline) membranes displayed a characteristic increase in permeability between reduced and half-oxidized states for neutrally charged phenol and negatively charged 4-hydroxybenzenesulfonate. In contrast, positively charged pyridine experienced decreased permeability through the membrane when poly(aniline) was switched from the reduced to the half-oxidized state. This behavior can be explained by a combination of oxidation-induced film swelling and the anion-exchange character of the positively charged membrane. The membrane composition was modified to include a fixed negative charge by the addition of poly(styrenesulfonate) during synthesis. The incorporation of this negatively charged component introduced cation-exchange character to the film and substantially reduced membrane permeability to 4-hydroxybenzenesulfonate in both oxidation states. In addition, increasing the fraction of poly(styrenesulfonate) in the membrane served to decrease film permeability for all species because of a densification of the membrane. This work demonstrates how both film composition and oxidation state can be used to tune the permeability of conducting polymer membranes.

Disciplines
Biological Engineering | Chemical Engineering | Chemistry

Comments
This article is from *Langmuir*22 (2006): 5925-5931, doi:10.1021/la060255b. Posted with permission.

Electrochemically Modulated Permeability of Poly(aniline) and Composite Poly(aniline)−Poly(styrenesulfonate) Membranes

D. L. Pile,† Y. Zhang, and A. C. Hillier*

Department of Chemical and Biological Engineering and Department of Chemistry, Iowa State University, Ames, Iowa 50011

Received January 26, 2006. In Final Form: April 10, 2006

The influence of oxidation state on the permeability of several probe molecules through conducting polymer membranes comprising composites of poly(aniline) and poly(styrenesulfonate) was examined in aqueous solution. Pure poly(aniline) membranes displayed a characteristic increase in permeability between reduced and half-oxidized states for neutrally charged phenol and negatively charged 4-hydroxybenzenesulfonate. In contrast, positively charged pyridine experienced decreased permeability through the membrane when poly(aniline) was switched from the reduced to the half-oxidized state. This behavior can be explained by a combination of oxidation-induced film swelling and the anion-exchange character of the positively charged membrane. The membrane composition was modified to include a fixed negative charge by the addition of poly(styrenesulfonate) during synthesis. The incorporation of this negatively charged component introduced cation-exchange character to the film and substantially reduced membrane permeability to 4-hydroxybenzenesulfonate in both oxidation states. In addition, increasing the fraction of poly(styrenesulfonate) in the membrane served to decrease film permeability for all species because of a densification of the membrane. This work demonstrates how both film composition and oxidation state can be used to tune the permeability of conducting polymer membranes.

Introduction

Intrinsically conducting polymers (ICPs) such as poly(aniline), poly(pyrrole), and poly(thiophene) have been exploited in a range of technologies because of their unique physical and electronic properties.[1−3] Their unusually high conductivities, for example, have been used to develop functional electronic devices,[4−8] conducting wires,[9,10] and electrostatic shielding. The sensitivity of their electronic properties to environmental stimuli has been exploited in the design of chemical and biological sensors.[11−18] In addition, ICPs exhibit several properties that are well-suited for membrane-based separations.[19]

ICP membranes have proven to be particularly effective for the separation of gases. For example, poly(aniline) membranes have exhibited extraordinarily high selectivity for the separation of gas mixtures, including O_2/N_2, H_2/N_2, and CO_2/CH_4.[20−22] Poly(pyrrole) and substituted poly(thiophene) membranes have also been exploited for gas separations.[23−26] The ability to modify the separation characteristics of ICPs by chemical or electrochemical doping demonstrates a key advantage in the ability to readily tune the properties of these polymer membranes.[21]

In liquids, ICP membranes have the added feature of being responsive to their environments, such as changing solution pH or applied electrochemical stimuli. Indeed, the ability to electrochemically modulate the properties of ICPs via oxidation or reduction provides a unique route to active control of their separation characteristics. Electrochemical processes in conducting polymers are frequently accompanied by changes in the local environment, such as changes in hydrophilicity, permselectivity, solute partitioning, solvent content, and volume swelling.[27,28] These properties can be used to modify separation characteristics when in the form of free-standing films or supported membranes.

* To whom correspondence should be addressed. E-mail: hillier@iastate.edu.

† Current address: Sandia National Laboratories, Albuquerque, NM 87185.

(1) Wallace, G. G.; Spinks, G. M.; Teasdale, P. R. *Conductive Electroactive Polymers. Intelligent Materials Systems*; Technomic Publishing Co., Inc.: Lancaster, PA, 1997.

(2) Skotheim, T. A., Elsenbaumer, R. L., Reynolds, J. R., Eds. *Handbook of Conducting Polymers*, 2nd ed.; Marcel Dekker: New York, 1998.

(3) Chandrasekhar, P. *Conducting Polymers, Fundamentals and Applications. A Practical Approach*; Kluwer Academic Publishers: Boston, MA, 1999.

(4) Yam, P. *Sci. Am.* **1995**, *273*, 82−87.

(5) Hohnholz, D.; MacDiarmid, A. G. *Synth. Met.* **2001**, *121*, 1327−1328.

(6) Kittlesen, G. P.; White, H. S.; Wrighton, M. S. *J. Am. Chem. Soc.* **1984**, *106*, 7389−7396.

(7) Mirkin, C. A.; Ratner, M. A. In *Annual Review of Physical Chemistry*; Strauss, H. L., Babcock, G. T., Leone, S. R., Eds.; Annual Reviews, Inc.: Palo Alto, CA, 1992; Vol. 43, pp 719−754.

(8) Dabke, R. B.; Singh, G. D.; Dhanabalan, A.; Lal, R.; Contractor, A. Q. *Anal. Chem.* **1997**, *69*, 724−727.

(9) Maia, D. J.; Zarbin, A. J. G.; Alves, O. L.; De Paoli, M. A. *Adv. Mater.* **1995**, *7*, 792−794.

(10) Shimidzu, T. *Pure Appl. Chem.* **1995**, *67*, 2039−2046.

(11) Rakow, N. A.; Suslick, K. S. *Nature* **2000**, *406*, 710−713.

(12) Massari, A. M.; Stevenson, K. J.; Hupp, J. T. *J. Electroanal. Chem.* **2001**, *500*, 185−191.

(13) Partridge, A. C.; Jansen, M. L.; Arnold, W. M. *Mater. Sci. Eng., C* **2000**, *12*, 37−42.

(14) McQuade, D. T.; Pullen, A. E.; Swager, T. M. *Chem. Rev.* **2000**, *100*, 2537−2574.

(15) Jin, Z.; Su, Y. X.; Duan, Y. X. *Sens. Actuator, B* **2000**, *71*, 118−122.

(16) Lu, W.; Nguyen, T. A.; Wallace, G. G. *Electroanalysis* **1998**, *10*, 1101−1107.

(17) Guiseppi-Elie, A.; Wallace, G. G.; Matsue, T. In *Handbook of Conducting Polymers*, 2nd ed.; Skotheim, T. A., Elsenbaumer, R. L., Reynolds, J. R., Eds.; Marcel Dekker: New York, 1998; pp 963−991.

(18) Partridge, A. C.; Harris, P.; Andrews, M. K. *Analyst* **1996**, *121*, 1349−1353.

(19) Pellegrino, J. In *Advanced Membrane Technology*; Li, N. N., Ed.; New York Academy of Sciences: New York, 2003; Vol. 984, pp 289−305.

(20) Anderson, M. R.; Mattes, B. R.; Reiss, H.; Kaner, R. B. *Science* **1991**, *252*, 1412−1415.

(21) Kuwabata, S.; Martin, C. R. *J. Membr. Sci.* **1994**, *91*, 1−12.

(22) Illing, G.; Hellgardt, K.; Wakeman, R. J.; Jungbauer, A. *J. Membr. Sci.* **2001**, *184*, 69−78.

(23) Parthasarathy, R. V.; Menon, V. P.; Martin, C. R. *Chem. Mater.* **1997**, *9*, 560−566.

(24) Liang, W. B.; Martin, C. R. *Chem. Mater.* **1991**, *3*, 390−391.

(25) Musselman, I. H.; Li, L.; Washmon, L.; Varadarajan, D.; Riley, S. J.; Hmyene, M.; Ferraris, J.; Balkus, K. J. *J. Membr. Sci.* **1999**, *152*, 1−18.

(26) Andreeva, D. V.; Pientka, Z.; Brozova, L.; Bleha, M.; Polotskaya, G. A.; Elyashevich, G. K. *Thin Solid Films* **2002**, *406*, 54−63.

(27) Focke, W. W.; Wnek, G. E.; Wei, Y. *J. Phys. Chem.* **1987**, *91*, 5813−5818.

(28) Orata, D.; Buttry, D. A. *J. Am. Chem. Soc.* **1987**, *109*, 3574−3581.

10.1021/la060255b CCC: $33.50
Published on Web 05/23/2006

Examples include the development of ion-gate membranes,[29−31] controlled release systems,[32−34] permselective membranes,[35,36] chromatography media,[37,38] and bilayer membranes.[39,40] However, challenges remain in designing functional membranes based upon ICPs. For example, the ability to achieve high selectivity while maintaining significant transport rates remains a major challenge. Improved selectivity has been addressed by the development of composite films and by the molecular imprinting of these polymers with specifically tailored chemistries.[41−43] Improvements in membrane structure have been partially addressed through careful polymerization methods,[23] the use of supported membranes,[44] and asymmetric/integrally skinned membrane processing.[45] Other outstanding problems include issues of long-term membrane stability and performance. In addition, there remains an insufficient understanding of the electrochemically induced transformations that occur in these films and their impact upon membrane permeability.

The work described here addresses the role of electrochemical modulation on aqueous-phase membrane transport to gain a better understanding of the role of membrane oxidation state as well as the impact of polymer composition on transport properties. We describe a detailed experimental study of the permeability of supported membranes comprised of pure poly(aniline) and poly(aniline) composites with poly(styrenesulfonate) (PSS). The influence of electrochemical modulation on membrane permeability is examined for several probe molecules of differing charge to deduce how polymer oxidation state and permeant charge influence transport rates. Also, the addition of PSS to the membrane composition is examined in view of its influence on separation characteristics and membrane morphology.

Experimental Section

Materials. ACS reagent grade concentrated sulfuric acid, aniline, pyridine (Aldrich Chemical Company, Inc., Milwaukee, WI), phenol (Alfa Aesar, Ward Hill, MA), 4-hydroxybenzenesulfonic acid sodium salt hydrate (Avocado Research Chemicals, Alfa Aesar, Ward Hill, MA), and poly(styrenesulfonic acid) sodium salt (PSS) (MW ≈ 70 000) (Polysciences, Inc., Warrington, PA) were used as received. All solutions were prepared in 18 MΩ deionized water (E-Pure, Barnstead, Dubuque, IA). The electrolyte solution used for all experiments was 0.5 M sulfuric acid. Probe molecules used during membrane permeation experiments included neutrally charged phenol (Ph), negatively charged 4-hydroxybenzenesulfonate (PhS^-), and pyridine ($PyrH^+$), which is protonated and positively charged in the solution pH values used for these experiments.

Membrane Electrodes. The membrane electrodes employed in these studies were of the asymmetric type. Membrane supports were fabricated by depositing 200 nm of gold (Ernest F. Fullam, Inc., Latham, NY) using a thermal evaporator (Bench Top Turbo III high vacuum evaporator, Denton Vacuum, LLC, Moorestown, NJ) onto the "filtration" side of a porous alumina membrane having 0.2 μm diameter pore channels (Anodisc 25, Whatman International Ltd., Maidstone, England). Electrical contact with the membrane was established by attaching a copper wire to the gold film with silver epoxy (Epo-Tek H20E, Epoxy Technology, Billerica, MA). This connection was reinforced and insulated with 5-Minute Epoxy (ITW Devcon, Danvers, MA) or epoxide (Buehler, Lake Bluff, IL).

The membranes were coated with polymer by electrodepositing a film onto the gold-coated membrane support. Poly(aniline) was electropolymerized from a solution of 0.1 M aniline in 0.5 M sulfuric acid by potential cycling using a potentiostat (Model 283, EG&G Instruments/Princeton Applied Research, Oak Ridge, TN). The potential was cycled between −0.2 and +1.15 V versus Ag/AgCl at 0.1 V s^{-1} for 10 cycles to create a film. The resulting polymer films were rinsed by scanning the potential between −0.2 and +1.15 V for one cycle and then between −0.2 and +0.5 V for 20 additional cycles in 0.5 M sulfuric acid. This procedure served to remove residual monomer and oxidation products. The same electrochemical parameters were used for making and rinsing composite membranes consisting of poly(aniline) and PSS. These were formed by electropolymerizing aniline in the presence of different concentrations of dissolved PSS. The aniline concentration was held constant at 0.1 M, while the three concentrations of PSS, on the basis of the sulfonate group, were 0.1 M (∼2 wt %), 0.25 M (∼5 wt %), and 0.50 M (∼10 wt %).

Membrane Permeability. A custom-made permeation cell was used for measurements of membrane permeability.[46] A freshly made polymer-coated membrane electrode was clamped into the permeation cell with the polymer film facing the source solution. A solution of 0.5 M sulfuric acid was then added to both the source and receiver sides of the cell. Reference (Ag/AgCl, 3 M NaCl) and counter (platinized mesh) electrodes were positioned on the source side, while the membrane served as the working electrode. Polypropylene stirring paddles on each side of the membrane kept the solutions well mixed. At the beginning of each permeation experiment, an aliquot of the permeant of choice (phenol, 4-hydroxybenzenesulfonate, or pyridine) was introduced to the source side to yield a concentration of 10 mM.

Membrane permeability was measured for both the reduced and half-oxidized states of the polymer film. To test the permeability of the two oxidation states, the membrane film was held at potentials of −0.150 V and then +0.500 V versus Ag/AgCl, corresponding to the reduced and half-oxidized states of poly(aniline). A fiber optic spectrophotometer (SD2000, Ocean Optics, Inc., Dunedin, FL) coupled with a capillary waveguide flow cell (LWCC II, World Precision Instruments, Inc., Sarasota, FL) was used to monitor the concentration of probe species in the receiver side as a function of time via ultraviolet absorbance. Flux (mol cm^{-2} s^{-1}) of the permeant across the membrane was determined by measuring the slope of the absorbance versus time curve and multiplying by the appropriate conversion factor. From the flux and the known concentration difference between the source and receiver sides of the cell, an overall mass transfer coefficient, *K*, for the permeant through the membrane assembly was determined. The mass transfer coefficient through just the membrane film was then determined by removing the component due to the uncoated membrane, as determined by a permeation experiment in the absence of the polymer film. Finally, permeability was determined by multiplying the membrane mass transfer coefficient by the film thickness. The film thickness for the various membranes was determined by averaging the value determined by cross-sectional scanning electron microscopy (SEM) imaging and that determined by taking the anodic peak current

(29) Burgmayer, P.; Murray, R. W. *J. Am. Chem. Soc.* **1982**, *104*, 6140−6142.
(30) Burgmayer, P.; Murray, R. W. *J. Electroanal. Chem.* **1983**, *147*, 339−344.
(31) Burgmayer, P.; Murray, R. W. *J. Phys. Chem.* **1984**, *88*, 2515−2521.
(32) Miller, L. L.; Zinger, B.; Zhou, Q. X. *J. Am. Chem. Soc.* **1987**, *109*, 2267−2272.
(33) Zhou, Q. X.; Miller, L. L.; Valentine, J. R. *J. Electroanal. Chem.* **1989**, *261*, 147−164.
(34) Zinger, B.; Miller, L. L. *J. Am. Chem. Soc.* **1984**, *106*, 6861−6863.
(35) Jüttner, K.; Ehrenbeck, C. *J. Solid State Electrochem.* **1998**, *2*, 60−66.
(36) Morita, M. *J. Appl. Polym. Sci.* **1998**, *70*, 647−653.
(37) Deinhammer, R. S.; Porter, M. D.; Shimazu, K. *J. Electroanal. Chem.* **1995**, *387*, 35−46.
(38) Deinhammer, R. S.; Shimazu, K.; Porter, M. D. *Anal. Chem.* **1991**, *63*, 1889−1894.
(39) Zhao, H.; Price, W. E.; Wallace, G. G. *J. Membr. Sci.* **1998**, *148*, 161−172.
(40) Zhou, D.; Zhao, H.; Price, W. E.; Wallace, G. G. *J. Membr. Sci.* **1995**, *98*, 173−176.
(41) Deore, B.; Chen, Z. D.; Nagaoka, T. *Anal. Chem.* **2000**, *72*, 3989−3994.
(42) Deore, B.; Freund, M. S. *Analyst* **2003**, *128*, 803−806.
(43) Shiigi, H.; Okamura, K.; Kijima, D.; Deore, B.; Sree, U.; Nagaoka, T. *J. Electrochem. Soc.* **2003**, *150*, H119−H123.
(44) Martin, C. R.; Liang, W.; Menon, V.; Parthasarathy, R.; Parthasarathy, A. *Synth. Met.* **1993**, *57*, 3766−3773.
(45) Wang, H. L.; Romero, R. J.; Mattes, B. R.; Zhu, Y. T.; Winokur, M. J. *J. Polym. Sci. Part B: Polym. Phys.* **2000**, *38*, 194−204.
(46) Pile, D. L.; Hillier, A. C. *J. Membr. Sci.* **2002**, *208*, 119−131.

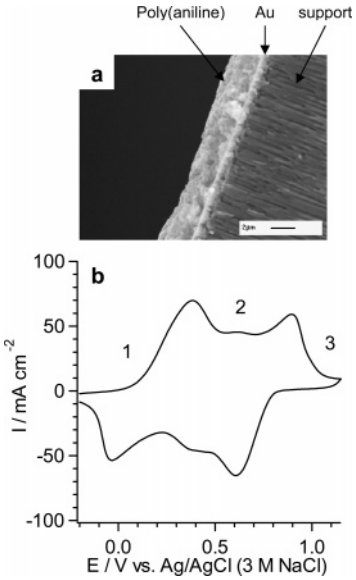

Figure 1. (a) SEM cross-sectional image of a poly(aniline) membrane electropolymerized from 0.1 M aniline/0.5 M H_2SO_4 on a porous alumina support. (b) Cyclic voltammogram of a poly(aniline) membrane in 0.5 M H_2SO_4. Regions 1, 2, and 3 denote the three oxidation states: (1) reduced, (2) half-oxidized, and (3) fully oxidized.

measured during potential cycling and converting it to thickness using an empirical correlation.[47,48]

SEM Imaging. Membrane thickness and morphology were imaged using a scanning electron microscope (JXA 840A, JEOL, Akishima, Tokyo, Japan). A LaB_6 filament at an accelerating voltage of 20 kV was used for all SEM imaging. Sections of the alumina support membrane both with and without deposited polymer were attached to an aluminum plate using double-sided, copper tape (No. 1182, 3M Electrical Products Division, Austin, TX). A section of each membrane was also fractured and mounted vertically on edge for imaging of its cross-section. A 20 nm layer of Au was then evaporated onto the samples to minimize the charging effects during SEM observation. Images were captured using Spirit software (Princeton Gamma-Tech, Inc., Princeton, NJ) in digital format.

Fourier Transform Infrared Spectroscopy. The compositions of the composite poly(aniline)/PSS films were determined using Fourier transform infrared (FTIR) reflectance spectra (see Supporting Information) captured using a commercial spectrometer (Magna-IR 550 FTIR, Nicolet, Madison, WI) interfaced with a microscope (Nic-Plan IR Microscope, Nicolet, Madison, WI). Spectra were acquired in the 650−4000 cm^{-1} region with 8 cm^{-1} resolution for the composite films and several reference samples. Reference samples consisted of pure poly(aniline) and PSS at various film thicknesses. Absorbance peaks at 1310 and 1041 cm^{-1} were used to measure the relative amounts of poly(aniline) and PSS, respectively. Calibration curves for both poly(aniline) and PSS were generated by monitoring peak height versus film thickness. The composite membrane films were prepared by electrodeposition onto gold-coated glass slides following the same procedure as that described earlier. The fraction of PSS in the composite films was estimated by calculating the amounts of both PSS and poly(aniline) in the films using the magnitude of the peaks at 1041 and 1310 cm^{-1}, respectively.

Results and Discussion

Supported membrane assemblies were constructed by electropolymerization of poly(aniline) onto a membrane support (vide supra).[46] Figure 1a depicts a cross-sectional SEM image of a typical membrane. In this example, a pure poly(aniline) film of ~3.2 μm thickness was formed on a gold-coated alumina membrane (Anopore) possessing collinear pores of ~0.2 μm diameter. Polymer thickness could be controlled by changing the number of potential scans or the scan rate during deposition, with thicker films resulting from an increased number of scans or a reduced scan rate.[46] Figure 1b depicts a cyclic voltammogram of the resulting poly(aniline) membrane in a solution of 0.5 M H_2SO_4. The current response shows the typical poly(aniline) behavior, where the regions denoted 1, 2, and 3 correspond to three distinct oxidation states. Region 1 reflects the fully reduced leucoemeraldine. Region 2 is the half-oxidized emeraldine. Region 3 is the fully oxidized pernigraniline. In each of these oxidation states, the polymer exhibits different physical, chemical, and electronic properties. For membrane applications, the most notable differences are associated with the charge, swelling, and stability of the films.

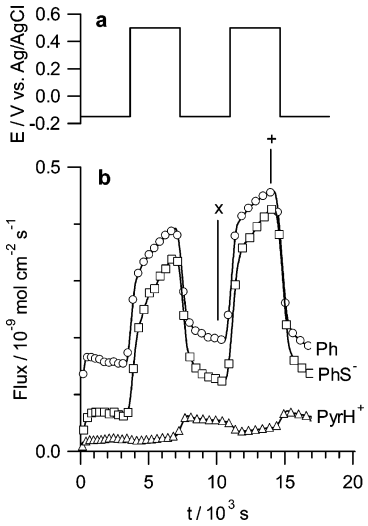

Figure 2. Summary of electrochemically modulated transport through a poly(aniline) membrane during a series of potential steps. (a) Electrochemical potential applied to membrane versus time to switch the film between reduced (−0.15 V) and half-oxidized (+0.5 V) states. (b) Measured flux rates for phenol (Ph, circle), 4-hydroxybenzenesulfonate (PhS^-, square), and pyridine ($PyrH^+$, triangle) during potential switching. The source concentration of each permeant was 10 mM. The symbols × and + denote where flux values were extracted for further analysis.

The influence of polymer oxidation state on membrane permeability was determined by monitoring the transport of several probe molecules across the membrane. Figure 2a depicts the potential waveform applied during a typical permeation experiment. The electrode potential was stepped between low and high values to switch the poly(aniline) between the reduced and half-oxidized states. Flux values were simultaneously recorded for three different permeants in successive experiments (Figure 2b). The initial increase in flux for all three species accompanies loading of the source compartment with the permeant. As the polymer's potential is switched between the reduced and half-oxidized states, modulation of the permeation rates occurs. Notably, the first cycle frequently behaves differently than subsequent cycles because of the loading of the film with permeant. Subsequent discussion focuses on changes observed during the second switching cycles, as shown in Figure 2.

For each permeant, there is a noticeable change in flux rates that accompanies the switching of the polymer oxidation state. Phenol exhibits a flux of ~0.2 × 10^{-9} mol cm^{-2} s^{-1} with the film in the fully reduced state (denoted by × in Figure 2b). Increasing the potential applied to the membrane results in a transition to a higher flux. The change can be characterized by an initially rapid rise that occurs within the first 50−100 s

(47) Johnson, B. J.; Park, S. M. *J. Electrochem. Soc.* **1996**, *143*, 1269−1276.
(48) Stilwell, D. E.; Park, S. M. *J. Electrochem. Soc.* **1989**, *136*, 427−433.

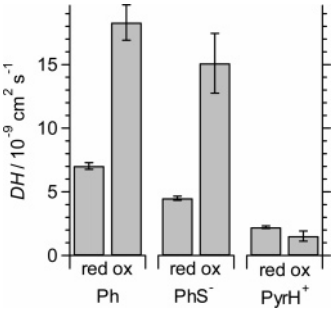

Figure 3. Permeabilities of various probe molecules through a poly(aniline) membrane in reduced (−0.15 V) and half-oxidized (+0.5 V) states.

following the step in potential. This rapid rise is followed by a slower increase in flux that proceeds in a continuous fashion as the potential remains held at 0.5 V. The maximum flux value recorded 60 min after the potential step (denoted by + in Figure 2b) is $\sim 0.45 \times 10^{-9}$ mol cm^{-2} s^{-1}, which is more than double that observed in the reduced state. Decreasing the potential applied to the membrane back to −0.15 V results in a rapid decrease in the measured flux. This is followed by a slow, steady decrease as the flux approaches its initial value. Thus, the observed transitions result in a reversible switching of the flux values between the reduced and half-oxidized states. Notably, switching the polymer to the fully oxidized state is accompanied by irreversible degradation of the polymer.[46]

Permeation experiments for 4-hydroxybenzenesulfonate show a similar but even larger change. An initially low flux of $\sim 0.14 \times 10^{-9}$ mol cm^{-2} s^{-1} is observed with the polymer in the reduced state. When a positive potential is applied, the flux of 4-hydroxybenzenesulfonate increases rapidly at first and then continues to increase slowly to a maximum near $\sim 0.42 \times 10^{-9}$ mol cm^{-2} s^{-1}, which is nearly triple the value in the reduced state. Decreasing the applied potential back to the reduced state decreases the flux of 4-hydroxybenzenesulfonate to its initial value.

Permeation experiments with pyridine show a distinctly different behavior. The initial flux value for pyridine with the polymer in the reduced state is low at $\sim 0.05 \times 10^{-9}$ mol cm^{-2} s^{-1}. When poly(aniline) is oxidized, the flux of pyridine decreases. This decrease occurs rapidly at first, with a low value approaching $\sim 0.03 \times 10^{-9}$ mol cm^{-2} s^{-1}, or almost half the value in the reduced state. When in the oxidized state, the pyridine flux increases gradually after the initial drop in a manner similar to the slow increase observed with both phenol and 4-hydroxybenzenesulfonate. Reducing the polymer film results in an increase in pyridine flux back to its initial value.

To quantitatively compare the behaviors of the various permeants, the measured flux values were converted into permeability (DH) to reflect the product of the diffusion coefficient (D) and the partition coefficient (H) associated with the polymer film. Figure 3 depicts permeability values for the various probe molecules through the 3.2 μm poly(aniline) film as measured 60 min after the corresponding potential value was applied. These permeabilities were determined by first fitting the measured flux for each permeant (N_j) to a two-film model that accounts for the concentration gradient of the permeant (ΔC_j) and mass transfer through both the polymer (k_M) and the gold-coated membrane support (k_S):

$$N_j = K_j \Delta C_j = \left(\frac{1}{1/k_M + 1/k_S} \right) \Delta C_j \qquad (1)$$

where the mass transfer coefficient through the support (k_S) was measured in a separate experiment in the absence of the poly(aniline) film. This was done to account for variations in k_S due to the slight reduction in pore size that occurred following evaporation of the gold layer on the support. Equation 1 was used to determine the mass transfer coefficient through the polymer membrane (k_M), which could then be converted to permeability by multiplying by the membrane thickness (L):

$$DH = k_M L \qquad (2)$$

As Figure 3 illustrates, the permeability of both phenol and 4-hydroxybenzenesulfonate increases substantially when poly(aniline) is switched from the reduced to the half-oxidized state. The increase in permeability for phenol is by a factor of ∼2.2, while, for 4-hydroxybenzenesulfonate, the increase is ∼3.4 times. In contrast, pyridine's permeability decreases through the oxidized polymer by a factor of ∼0.7. A consideration of the various processes that occur in the polymer during oxidation and reduction can be used to explain these behaviors.

Phenol is neutrally charged, and thus no charge repulsion or attraction forces are expected to influence its permeability. As a consequence, modulation of its permeability can be interpreted primarily in terms of the potential-induced swelling and shrinking of the polymer film that occurs during oxidation and reduction. Thus, the increase in permeability through the oxidized film is due to an increased openness of the polymer, which reduces its resistance to mass transfer. 4-hydroxybenzenesulfonate differs slightly from phenol in that it has a net negative charge, which allows it to serve as a charge-compensating ion for the oxidized film. Thus, a greater increase in permeability for 4-hydroxybenzenesulfonate through the oxidized polymer would be expected and is observed. The permeability of pyridine contrasts markedly with that of phenol and 4-hydroxybenzenesulfonate. While the neutral and negatively charged species exhibit enhanced permeation through the oxidized polymer, the permeation of positively charged pyridine is reduced. This is a consequence of the charge repulsion experienced by this molecule when it encounters the oxidized polymer.

The transformation of poly(aniline) between the reduced and half-oxidized states results in the insertion of positive charge into the polymer matrix, which is accompanied by the incorporation of solvated anions and leads to bulk volume swelling. Both of these phenomena favor the increased permeability of neutral and negatively charged species through the oxidized membrane. However, these phenomena have competing effects on a positively charged permeant. The oxidized film will repel pyridine because of its positive charge, but its swollen state will allow a greater transport rate. The net result is a reduction in the permeation rate of pyridine through the oxidized film, which suggests that electrostatic repulsion is the dominant effect.

Several additional features are noted with regard to the switching mechanism of the polymer membrane. The large change in flux at the beginning of each potential step likely reflects the rapid swelling or shrinking of the film that accompanies the insertion or removal of charge in the film. The direction of the change in flux during this process is related to the charge on the permeant, with neutral and negative species increasing and positive species decreasing upon switching the film from the reduced to the half-oxidized state. This initially rapid change in permeability is then followed by a more gradual and longer time-scale process, which shows a characteristic dependence on the oxidation state of the polymer, but is independent of the charge of the permeant. The change in flux has a shallow, positive slope during the oxidation step and a shallow, negative slope during

the reduction step for all permeants. This suggests that this process is a longer time-scale relaxation that involves additional swelling (during oxidation) or shrinkage (during reduction) of the film. At longer time-scales, the pathway for permeant transport through the polymer film becomes more open after the initial swelling and more closed after the initial shrinking.

Most studies of the electrochemical switching of conducting polymers have involved fairly rapid potential sweeping methods. For example, early studies of ion ingress and egress using quartz crystal microbalance (QCM) reported that, in sweeping the potential of poly(aniline) from the reduced state to the half-oxidized state, proton egress dominates in the early stages of film oxidation followed by anion ingress at more positive potentials.[28] However, the scan rates employed in those studies were too rapid to identify long-term relaxation processes. A few reports have described relaxation effects. For example, long time-scale potential step experiments using the QCM demonstrated that >80% of the mass change measured following a potential step occurred within the first second after the step in potential.[49,50] This initial change was attributed primarily to anion ingress. After this large initial change, a slower mass increase was observed over a period of 10−1000 s after the potential step. This slow increase was attributed to a slow, logarithmic-type relaxation in the film allowing the uptake of additional ions. The initial stages after the potential step are characterized by the fast movement of polymer chains due to charging of the film. Subsequently, the polymer chains reorganize over time, thus permitting a more open structure for the oxidized form and acquiring a more compact structure for the reduced form. The direction of the change in flux for this long-term process is in accordance with this type of relaxation. A long-term increase in flux is observed for all three permeants with the polymer in the oxidized state, which is consistent with the polymer chains reorganizing to provide greater swelling. A long-term decrease in flux is observed for all permeants during the reduction step, which is consistent with the additional shrinkage of the film that occurs as the polymer chains readjust and create a more densely packed film.

A second series of experiments was performed to study the influence of polymer composition on permeation. For these studies, a series of poly(aniline) films were prepared in the presence of PSS to create composite membranes. The addition of PSS to the deposition solution results in the formation of poly(aniline) films that contain a fixed negative charge due to the incorporation of PSS during electropolymerization. Figure 4a depicts a supported poly(aniline) film formed using the same deposition procedures as those used to form the unmodified film, but in the presence of 0.25 M PSS in the deposition solution. This film is noticeably thinner than that grown in the absence of PSS, with a thickness of only ∼1.3 μm. Nevertheless, the electrochemical behavior of the composite poly(aniline)−PSS film shows characteristics similar to those of unmodified poly(aniline) (Figure 4b). Two distinct pairs of oxidation and reduction peaks appear, reflecting the formation of all three polymer oxidation states. The total current measured during cycling of this composite polymer is ∼60% of the unmodified film, which is consistent with the reduced thickness of the polymer.

Several additional composite films were also prepared in an attempt to investigate a range of composite films. Figure 5a depicts thickness measurements for a series of membranes created by electropolymerization from a 0.1 M aniline/0.5 M H_2SO_4 solution containing 0, 0.1, 0.25, and 0.5 M PSS. The addition of PSS to the deposition solution served to decrease both the growth rate and the thickness of the resulting films as well as to modify the film compositions. The relative PSS content in the composite films was determined using reflectance FTIR (Figure 5b). At low PSS content in solution between 0 and 0.25 M, a linear increase in the PSS fraction is observed in the resulting films. At the highest PSS content (0.5 M), a decrease in both the film thickness and the PSS content is observed as the film growth rate is severely reduced.

The addition of PSS to the membranes also had a significant impact upon the polymer morphology. Figure 6 depicts several plan-view images of the surfaces of the various polymer films.

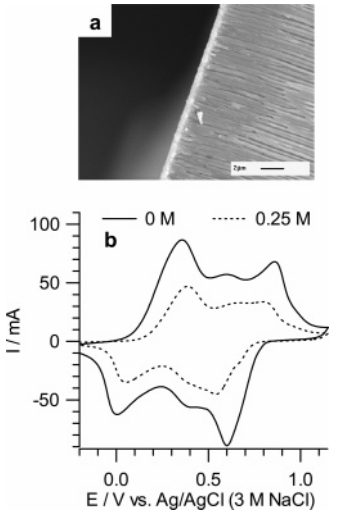

Figure 4. (a) SEM cross-sectional image of a poly(aniline)−PSS membrane formed from a solution of 0.1 M aniline and 0.25 M PSS on a porous alumina support. (b) Cyclic voltammograms of poly(aniline) (solid line) and composite poly(aniline)−PSS (dashed line) membranes in 0.5 M H_2SO_4.

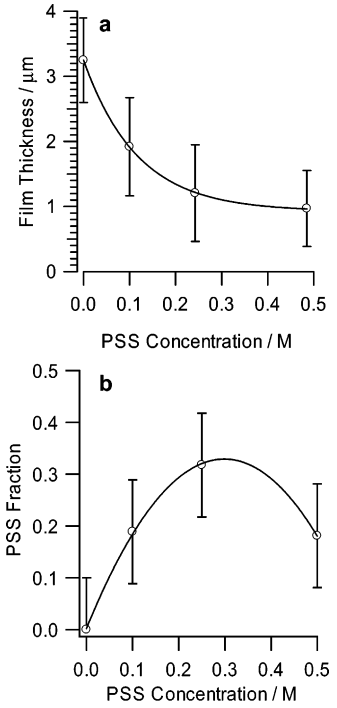

Figure 5. (a) Thickness of poly(aniline)−PSS membranes as a function of PSS concentration in the deposition solution. (b) Fraction of PSS in composite membranes as determined by FTIR reflectance spectra.

(49) Pruneanu, S.; Csahok, E.; Kertesz, V.; Inzelt, G. *Electrochim. Acta* **1998**, *43*, 2305−2323.
(50) Inzelt, G. *Electrochim. Acta* **2000**, *45*, 3865−3876.

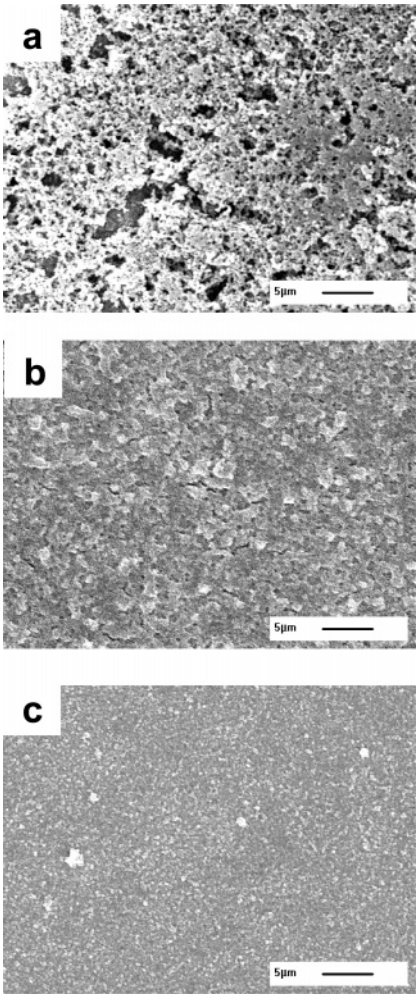

Figure 6. SEM plan-view images of composite poly(aniline)−PSS membranes fabricated from solutions containing (a) 0 M, (b) 0.1 M, and (c) 0.25 M PSS.

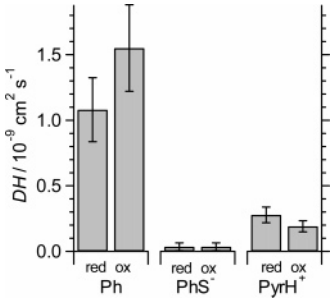

Figure 7. Permeabilities of various probe molecules through a poly(aniline)−PSS membrane, fabricated from a 0.25 M PSS solution, in reduced (−0.15 V) and half-oxidized (+0.5 V) states.

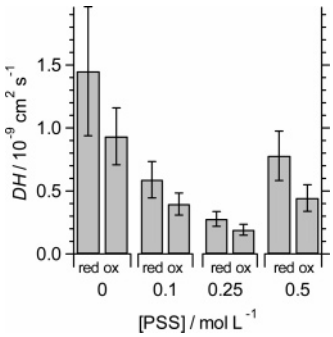

Figure 8. Permeability of pyridine ($PyrH^+$) through composite poly(aniline)−PSS membranes in reduced and half-oxidized states as a function of polystyrene composition in the deposition solution.

Unmodified poly(aniline) exhibits a characteristic loose and fibrillar morphology with large open regions and a highly porous structure (Figure 6a). The addition of PSS changes the morphology substantially. Figure 6b shows a denser grainlike structure for the composite poly(aniline)−PSS film grown from 0.1 M PSS. Far less porosity is observed in the film. The 0.25 M PSS film (Figure 6c) has an even more dense and uniform structure with no noticeable pores or cracks. For the 0.5 M PSS film (not shown), the film thickness is so low that features of the microporous support appear through the polymer, suggesting that a discontinuous layer is formed.

Permeation experiments with these PSS-modified poly(aniline) membranes show significant differences from that of unmodified poly(aniline). Figure 7 depicts permeabilities for phenol, 4-hydroxybenzenesulfonate, and pyridine for a membrane prepared from 0.25 M PSS in the reduced and half-oxidized states. The measured permeabilities are considerably lower, by a factor of ∼6, over the unmodified polymer. Since the permeability should be independent of film thickness, the reduced permeability reflects the effect of incorporated PSS on film charge, morphology, and density. Results for phenol continue to show a switching behavior in which permeability through the oxidized polymer is greater than that through the reduced form. However, the magnitude of the change is reduced to ∼1.5 times. This indicates that the composite polymer continues to undergo film swelling, but not to the magnitude displayed by pure poly(aniline). This is likely the result of the fixed negative charge in the film via PSS incorporation, which would serve to reduce the degree of anion ingress and the associated swelling that occurs during oxidation of the film. The permeability of 4-hydroxybenzenesulfonate has decreased to near zero for both reduced and oxidized states. Rejection of the negatively charged 4-hydroxybenzenesulfonate from the polymer is consistent with a cation exchange character, which the film should now possess due to the fixed negative charges from PSS. The permeability of pyridine appears to be very similar to that observed for the pure poly(aniline) film in that it is enhanced in the reduced state over the oxidized state. This behavior reflects a competition between the nature of the reduced film, which is more compact but is a pure cation exchanger with the fixed PSS charge, and the oxidized film, which is swollen but zwitterionic in that it contains both negative charge due to bound PSS and positive charge due to the charge injected during oxidation.

A final set of measurements illustrates the impact of changing PSS content on the permeability to pyridine (Figure 8). For each film examined, the permeability of pyridine continued to be modulated by changing the oxidation state of the membrane, with a higher value being recorded with the film in the reduced state. In addition, the permeabilities in both the reduced and oxidized states decreased with decreasing film thickness down to a thickness of ∼1.2 μm for the 0.25 M PSS film. An explanation for this trend is suggested by the SEM images of the film surfaces. The decrease in porosity and increase in the compactness of the film with increasing PSS content is a reasonable explanation for the decreased permeability of the membranes. As the films become more compact, there is increased resistance to mass transfer across the membrane. Thus, PSS serves both as a source of fixed negative charge to change the ion exchange character of the membrane and also as a modifier of film growth to produce denser films.

Both of these features influence the permeation characteristics of the resulting supported membranes.

Conclusions

This work demonstrates the ability to tune the permeation characteristics of supported conducting polymer membranes by controlling both the oxidation state of the polymer and the composition of the membranes. A combination of injected charge, short- and long-term film swelling, and the presence of fixed charges in the film influence the ability to electrochemically modulate the permeability of several probe molecules. Also, the addition of PSS as a film modifier was seen to change the morphology of the membranes, with increasing PSS content creating a denser film showing reduced permeability.

Acknowledgment. The authors gratefully acknowledge the National Science Foundation (CTS-0405442) and Iowa State University for partial support of this work.

Supporting Information Available: Infrared spectra and calibration curves are available for the various polymer films. This material is available free of charge via the Internet at http://pubs.acs.org.

Note Added after ASAP Publication. This manuscript was originally published on the Web May 23, 2006. The manuscript was reposted May 24, 2006 with corrected values of the reduced-state voltages given in the figure captions of Figures 2, 3, and 7.

LA060255B